

# $\alpha 3$ -Integrins are required for hippocampal long-term potentiation and working memory

Chi-Shing Chan,<sup>1</sup> Jonathan M. Levenson,<sup>2,3,6</sup> Partha S. Mukhopadhyay,<sup>3</sup> Lin Zong,<sup>1</sup> Allan Bradley,<sup>4,7</sup> J. David Sweatt,<sup>2,8</sup> and Ronald L. Davis<sup>1,5,9</sup>

<sup>1</sup>Department of Molecular and Cellular Biology, Baylor College of Medicine, Houston, Texas 77030, USA; <sup>2</sup>Department of Neuroscience, Baylor College of Medicine, Houston, Texas 77030, USA; <sup>3</sup>Department of Pharmacology and The Waisman Center, University of Wisconsin School of Medicine & Public Health, Madison, Wisconsin 53706, USA; <sup>4</sup>Department of Molecular and Human Genetics, Baylor College of Medicine, Houston, Texas 77030, USA; <sup>5</sup>Menninger Department of Psychiatry and Behavioral Sciences, Baylor College of Medicine, Houston, Texas 77030, USA

Integrins comprise a large family of heterodimeric, transmembrane cell adhesion receptors that mediate diverse neuronal functions in the developing and adult CNS. Recent pharmacological and genetic studies have suggested that  $\beta 1$ -integrins are critical in synaptic plasticity and memory formation. To further define the role of integrins in these processes, we generated a postnatal forebrain and excitatory neuron-specific knockout of  $\alpha 3$ -integrin, one of several binding partners for  $\beta 1$  subunit. At hippocampal Schaffer collateral-CA1 synapses, deletion of  $\alpha 3$ -integrin resulted in impaired long-term potentiation (LTP). Basal synaptic transmission and paired-pulse facilitation were normal in the absence of  $\alpha 3$ -integrin. Behavioral studies demonstrated that the mutant mice were selectively defective in a hippocampus-dependent, nonmatch-to-place working memory task, but were normal in other hippocampus-dependent spatial tasks. The impairment in LTP and working memory is similar to that observed in  $\beta 1$ -integrin conditional knockout mice, suggesting that  $\alpha 3$ -integrin is the functional binding partner for  $\beta 1$  for these processes in the forebrain.

Learning requires adaptive changes at certain synapses in response to environmental stimuli. The identification and characterization of molecules that underlie these experience-dependent synaptic changes has been one of the major goals in neuroscience research. Studies over the past decade have identified a plethora of proteins that are required for different forms of synaptic plasticity and different types of memory. Among them are the integrins, which are cell adhesion receptors involved in cell-cell and cell-extracellular matrix interaction (van der Flier and Sonnenberg 2001; Hynes 2002).

Integrins are heterodimeric transmembrane proteins consisting of noncovalently linked  $\alpha$  and  $\beta$  subunits. Currently, 18  $\alpha$  and eight  $\beta$  subunits are identified, forming over 22 integrin molecules in nature. In mammals, the majority of these integrins have been shown to be expressed in the brain (Pinkstaff et al. 1998, 1999; Chan et al. 2003; www.brain-map.org). For example, expression of  $\beta 1$  subunit is overlapped with its known binding partners  $\alpha 3$ ,  $\alpha 5$ ,  $\alpha 7$ ,  $\alpha 8$ , and  $\alpha V$  in the cortex and with  $\alpha 1$ ,  $\alpha 3$ ,  $\alpha 4$ ,  $\alpha 5$ ,  $\alpha 6$ ,  $\alpha 7$ ,  $\alpha 8$ , and  $\alpha V$  in the hippocampus. Accumulating evidence has shown that integrins, in general, are involved in multiple forms of synaptic plasticity and memory formation. For example, in *Drosophila*, mutations in *Volado*, the gene encoding the  $\alpha PS3$ -integrin, result in significant defects in two forms of  $Ca^{2+}$ -dependent short-term facilitation, paired-pulse facilitation (PPF), and frequency-dependent short-term facilitation and in post-tetanic potentiation (PTP) at the neuromuscular junction (Rohrbough et al. 2000). *Volado* mutants were also reported as

impaired in memory after olfactory classical conditioning (Grotewiel et al. 1998). In rodents,  $\alpha 3$ - and  $\beta 1$ -containing integrins have been implicated in negatively regulating rebound potentiation in the cerebellum, a distinct type of long-lasting potentiation induced by postsynaptic depolarization at the GABAergic synapses between inhibitory interneurons and a Purkinje neuron (Kawaguchi and Hirano 2006). At the hippocampal Schaffer collateral synapses, integrin antagonists such as RGD-containing peptides, function blocking antibodies, and disintegrins, which are small, high binding affinity, RGD-containing integrin inhibitors found in various snake venoms, are known to block the consolidation of LTP (Bahr et al. 1997; Stäubli et al. 1998; Chun et al. 2001; Kramár et al. 2002).

More recently, genetic studies have been employed to distinguish the specific roles for individual integrin subunits in mice. Animals with a forebrain-specific loss of  $\beta 1$ -integrin exhibit impaired hippocampal LTP (Chan et al. 2006; Huang et al. 2006). PPF in the hippocampus is also abnormal at certain inter-pulse intervals in  $\alpha 3$ - and  $\alpha 5$ -integrin double heterozygous mutant adults (Chan et al. 2003) and in animals that lack the postnatal expression of  $\beta 1$ -integrin (Huang et al. 2006). Behavioral studies on the forebrain-specific  $\beta 1$ -integrin knockouts have revealed a selective impairment in hippocampus-dependent working memory but not in other hippocampus-dependent tasks such as spatial memory or the memory of conditioned fear (Chan et al. 2006). These studies have revealed a specific behavioral role for  $\beta 1$ -integrins in working memory, a phenotype that is very rare among mouse knockouts. However, it is unclear how  $\beta 1$ -integrins function at the cellular level in the service of working memory. In addition, the  $\alpha$ -integrin partner that functions along with  $\beta 1$ -integrin for normal working memory has remained unknown, and its identification has been challenging in part due to the number of potential candidates.

In an attempt to identify the functional partner for  $\beta 1$ -

**Present addresses:** <sup>6</sup>Galenea Corp., Cambridge, MA 02139, USA; <sup>7</sup>Wellcome Trust Sanger Institute, Hinxton, Cambridge CB10 1SA, UK; <sup>8</sup>Department of Neurobiology, University of Alabama at Birmingham, Birmingham, AL 35282-9191, USA.

<sup>9</sup>Corresponding author.

E-mail rdavis@bcm.tmc.edu; fax (713) 798-8005.

Article is online at <http://www.learnmem.org/cgi/doi/10.1101/lm.648607>.

integrin, we chose  $\alpha 3$ -integrin as a potential candidate based on its expression pattern in the forebrain (Pinkstaff et al. 1998; Chan et al. 2003) and the observed deficit in hippocampal LTP in heterozygous  $\alpha 3$ -integrin mutants (Chan et al. 2003). In the present study, we examined the roles of  $\alpha 3$ -integrin in physiological and behavioral functions by generating a postnatal- and forebrain-specific knockout using the Cre/loxP recombination system. Our results show that hippocampal LTP is severely defective in these conditional knockout animals, while basal synaptic transmission, PPF, and long-term depression (LTD) remain intact. Behavioral experiments reveal that the  $\alpha 3$ -integrin conditional mutants exhibit impaired performance in a hippocampus-dependent non-match-to-place working memory task but normal performance in other hippocampus-dependent and -independent behavioral tasks. The impairment in LTP and working memory is very similar to phenotypes displayed by the  $\beta 1$ -integrin conditional knockout, strongly suggesting that  $\alpha 3$ -integrin is the functional binding partner of the  $\beta 1$  subunit for working memory and LTP.

## Results

### Generation of forebrain-specific, knockout of the $\alpha 3$ -integrin gene

To delineate the *in vivo* neuronal functions and the role of  $\alpha 3$ -integrin in learning and memory, we generated mice with a floxed allele of  $\alpha 3$ -integrin [ $f(\alpha 3)$ ] to use for constructing a postnatal, forebrain-specific and excitatory neuron-specific  $\alpha 3$ -integrin conditional knockout [ $f(\alpha 3)$ KO]. A construct was created in which two loxP sites were inserted into introns flanking exons 11–18, which encodes amino acid residues 491–768 (Fig. 1A). Cre-mediated recombination between these two loxP sites leads to a non-sense mutation from direct splicing of exon 10 to exon 19, resulting in a truncated peptide, predicted to be missing more than half of the wild-type sequence, including those that encode the transmembrane and the cytoplasmic domains. The second loxP site was followed immediately by a neomycin-thymidine kinase-loxP cassette. Targeted ES cell clones produced via homologous recombination with the construct and missing the TK-neo cassette produced by Cre-mediated recombination between the second and the third loxP sites were selected to generate germline-transmitting chimeras (Fig. 1B). Heterozygous mice carrying the  $f(\alpha 3)$  allele were out-crossed to wild-type C57BL/6 mice for six generations to minimize the potential effects of genetic background on physiological and behavioral testing described below.

To inactivate the  $\alpha 3$ -integrin gene specifically in the forebrain excitatory neurons, a transgene carrying Cre recombinase

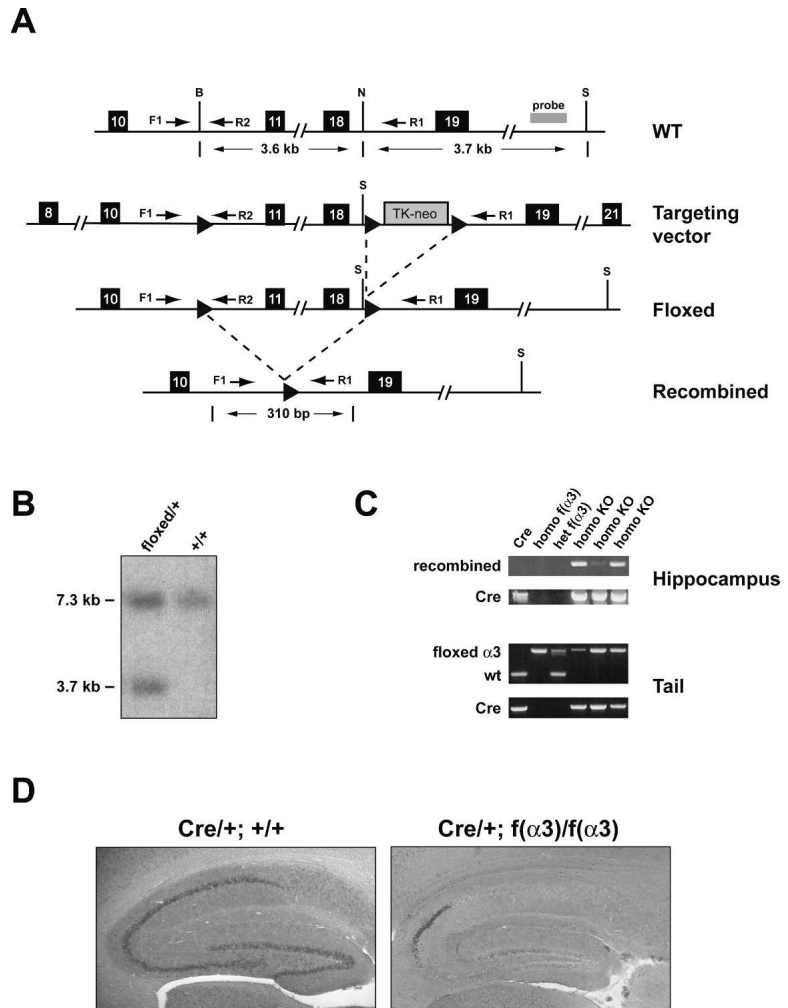


**Figure 1.** Generation of  $f(\alpha 3)$  knockout mice. (A) Schematic diagram of a portion of the  $\alpha 3$ -integrin genomic region, the targeting vector, the targeted locus, and the recombined allele. The numbers in the solid dark boxes mark the positions of exons. The 34-bp loxP sequence is indicated by arrowheads. The probe used for Southern blot analysis of the ES cell DNA in B is indicated. Dotted lines indicate Cre-mediated recombination events. B, BglII; N, NheI; and S, SpeI. (B) Southern blot analysis of genomic DNA isolated from Cre-transfected ES cells double-digested with BglII and SpeI and probed with an external probe as indicated in A. The probe detected a 7.3-kb BglII-SpeI fragment in wild-type (+/+) and heterozygous (+/-) cells, and a 3.7-kb SpeI fragment only in the heterozygous cells. (C) PCR analyses of hippocampal and tail genomic DNA isolated from Cre (Cre/+; +/+), homo  $f(\alpha 3)$  [+/+;  $f(\alpha 3)/f(\alpha 3)$ ], het  $f(\alpha 3)$  [+/+;  $f(\alpha 3)/+$ ], and three different homo KO [Cre/+;  $f(\alpha 3)/f(\alpha 3)$ ] mice. In the hippocampus, Cre-mediated recombination of the  $f(\alpha 3)$  allele was observed only in the presence of Cre product. (D) In situ hybridization of  $\alpha 3$ -integrin mRNA expression in the hippocampus of Cre/+ control (left) and  $f(\alpha 3)$ KO animals (right). The  $\alpha 3$ -integrin gene expression in CA1 cells was undetectable and was greatly reduced in CA3 and dentate gyrus cells.

driven by the  $\alpha$ -CaMKII promoter (Tsien et al. 1996) was introduced into the genome of  $f(\alpha 3)$  homozygous mice. PCR analyses of genomic DNA isolated from the hippocampus of these and control animals confirmed the occurrence of the predicted Cre-dependent recombination between the two loxP sites in the  $f(\alpha 3)$ KO animals, although the efficiency of recombination may differ among the mutants (Fig. 1C, lanes 4–6). Furthermore, we confirmed by *in situ* hybridization with a probe whose sequence was inside the deleted region that mRNA expression of  $\alpha 3$ -integrin was undetectable in CA1 neurons and was greatly reduced in CA3 and dentate gyrus cells (Fig. 1D).

Since integrins provide a physical link between the extracellular matrix and the intracellular cytoskeletal networks, we examined whether the postnatal loss of  $\alpha 3$ -integrin compromises

the structural integrity of the neurons. No detectable alterations were observed in CNS gross anatomy in the  $f(\alpha 3)$ KO animals at the level of light microscopy (data not shown). Next we examined more than 1100 axospinous and axodendritic synaptic contacts from the stratum radiatum of the hippocampal CA1 region using electron microscopy and detected no morphological differences upon comparing synapses of  $f(\alpha 3)$ KO ( $Cre/+; f(\alpha 3)/f(\alpha 3)$ ) animals with  $Cre$  ( $Cre/+; +/+$ ) control animals (Fig. 2A). We also compared the distribution of synapse size and the width of the synaptic cleft for the two groups. There was no statistical difference between the two groups in either the length ( $Cre/+$ ,  $193 \pm 2$  nm;  $f(\alpha 3)$ KO,  $192 \pm 2$  nm;  $P = 0.59$ ,  $t$ -test) of the synapses (Fig. 2B) or in the width ( $Cre/+$ ,  $14.5 \pm 0.3$  nm;  $f(\alpha 3)$ KO,  $15.38 \pm 0.4$  nm;  $P = 0.06$ ,  $t$ -test) of the synaptic clefts (Fig. 2C), indicating that synaptic structures remain intact in the  $f(\alpha 3)$ KO animals.

### Hippocampal LTP is impaired in $f(\alpha 3)$ KO mice

To investigate the physiological consequences of loss of  $\alpha 3$ -integrin in the adult forebrain, we performed electrophysiological recordings from hippocampal neurons stimulated via the Schaffer collateral pathway. We first measured the CA1 field excitatory post-synaptic potentials (fEPSPs) in hippocampal slices prepared from the  $f(\alpha 3)$ KO as a function of fiber volley amplitude, and observed no significant difference in basal synaptic transmission between  $f(\alpha 3)$  KOs and their control littermates (Fig. 3A).

We next investigated the effects of  $\alpha 3$ -integrin inactivation on synaptic plasticity. PPF is a transient form of pre-synaptic-dependent short-term plasticity believed to be the result of enhanced probability of synaptic vesicle release. This phenomenon occurs with the facilitation of a closely timed second stimulus primarily due to residual calcium remaining from the first stimulation (Wu and Saggau 1994). Analysis of PPF did not reveal significant differences between the  $f(\alpha 3)$ KO and the control animals over a range of intervals between 20 and 300 msec (Fig. 3B). Similar to PPF, PTP is an enhancement of synaptic transmission due to the continuing action of residual presynaptic calcium but occurs from extensive high-frequency or tetanic presynaptic activity and persists longer. Consistent with the PPF result,  $f(\alpha 3)$ KO slices showed indistinguishable PTP from the control slices (Fig. 3C). Together these results suggest that  $\alpha 3$ -integrin is not significantly involved in the regulation of baseline neurotransmitter release or in several types of short-term synaptic plasticity.

In contrast, NMDA receptor-dependent LTP was severely impaired in the  $f(\alpha 3)$ KO mice. Whereas two trains of high frequency stimulation (HFS; 100 Hz) elicited robust LTP in the wild-type

slices, they failed to generate an appreciable amount of LTP throughout the entire recording period in the  $f(\alpha 3)$ KO slices (Fig. 3D). In addition, a similar deficit in LTP remained in the  $f(\alpha 3)$ KOs when saturating amounts of HFS (four trains of 100 Hz stimulation) were used to generate the LTP (Fig. 3E), indicating that a stronger stimulation did not compensate for the loss of  $\alpha 3$ -integrin subunit. Measurement of the area under the curve for each tetanus in the robust LTP induction paradigm indicated no significant differences (Fig. 3F), suggesting the synaptic mechanisms involved in the induction of LTP are normal in  $f(\alpha 3)$ KO mice. Moreover, mGluR-dependent LTD was indistinguishable in the  $f(\alpha 3)$ KO slices from the controls (Fig. 3G), indicating that  $\alpha 3$  integrin is not essential for this type of long-term plasticity and that loss of  $\alpha 3$  integrin did not result in the complete loss of the ability of synapses to exhibit plasticity.

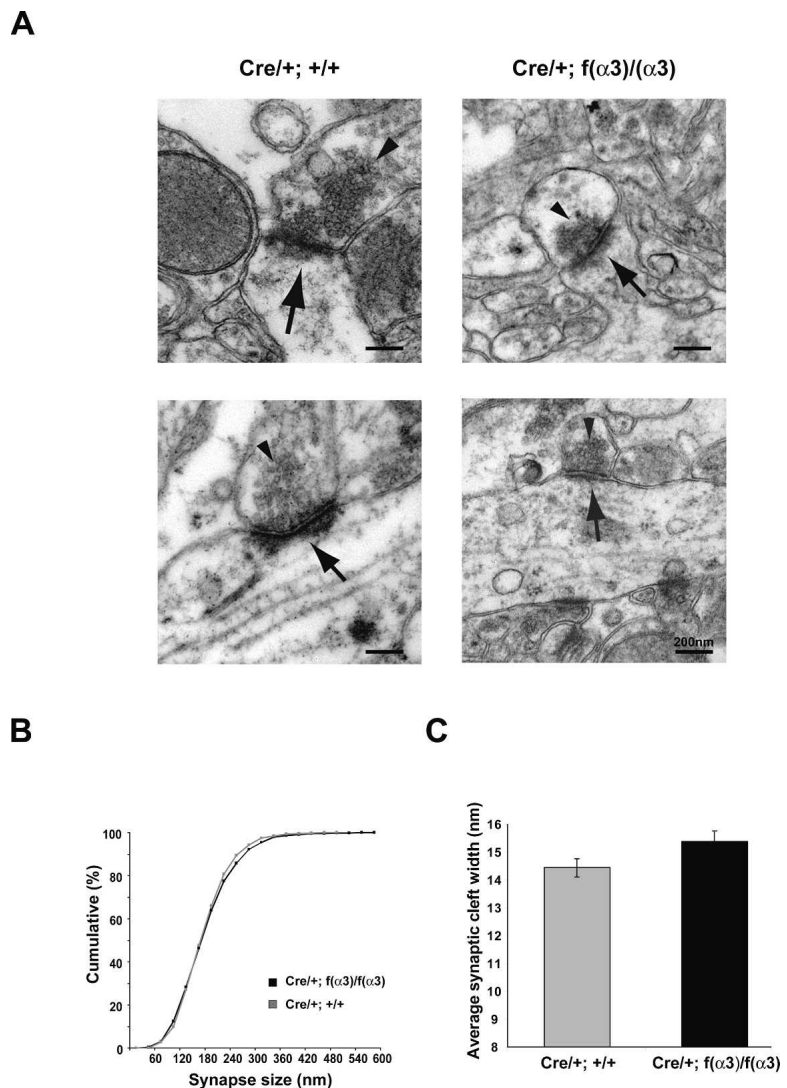


**Figure 2.** Normal synaptic ultrastructure in  $\alpha 3$ -integrin knockouts. (A) Representative electron micrographs of axospinous (*upper panels*) and axodendritic (*lower panels*) synaptic contacts in the hippocampal CA1 stratum radiatum region of  $Cre$  control (*left column*) and  $f(\alpha 3)$ KO (*right column*) animals. No detectable morphological difference in either type of contact was detected between the two genotypes at either presynaptic (arrow heads) or postsynaptic (arrows) terminals. Scale bars, 200 nm. (B) Cumulative frequency plot of synapse size in the CA1 stratum radiatum measured as the length of the postsynaptic density. Synapse size distribution of  $f(\alpha 3)$ KOs was indistinguishable from the  $Cre/+$  control animals. (C) Bar plot of the average width of the synaptic cleft, measured by dividing the area of the gap juxtaposing the PSD by the length of the PSD. No significant difference was found between the  $f(\alpha 3)$ KOs and the  $Cre/+$  control animals.

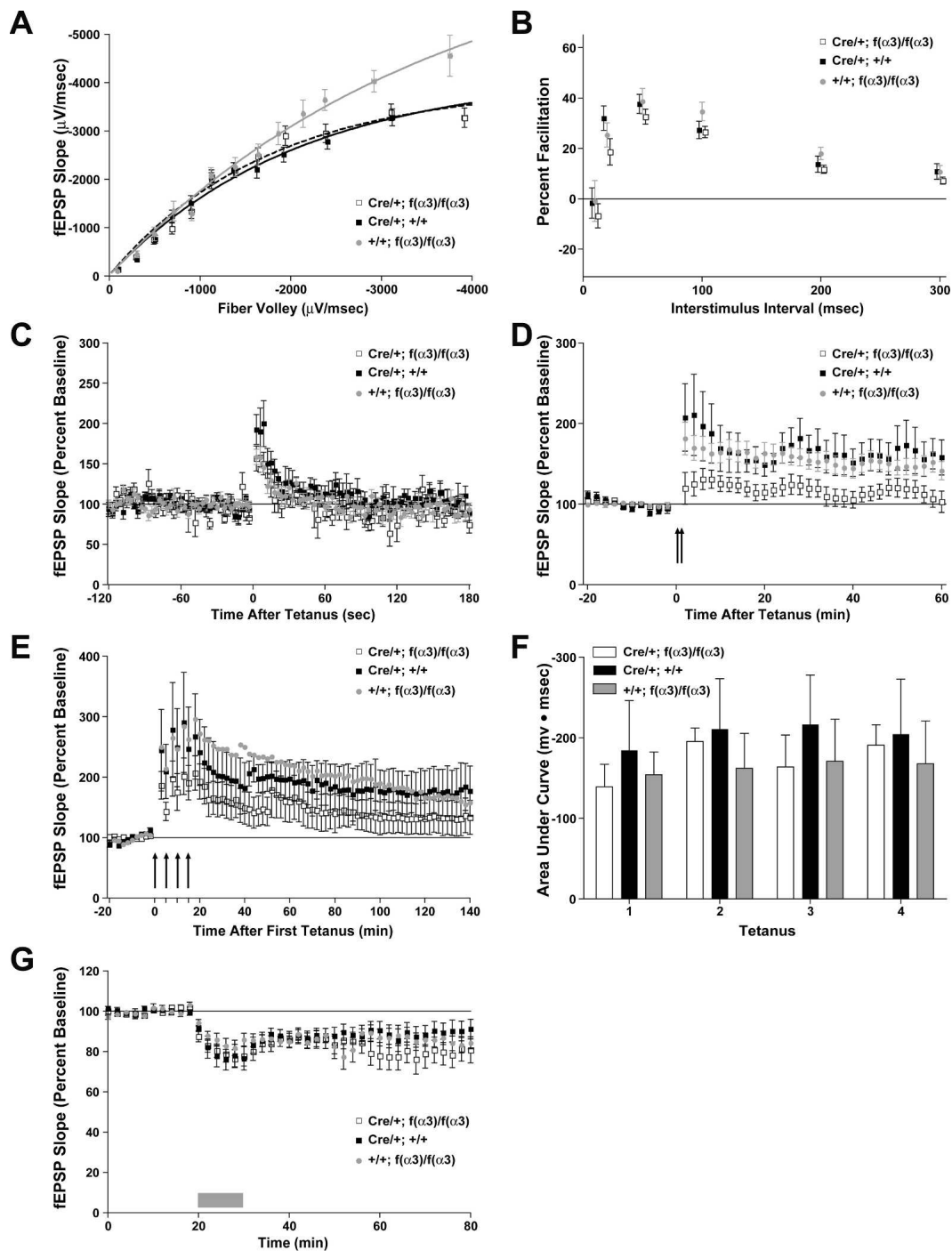


**Figure 3.** Deficits in LTP are associated with the loss of  $\alpha 3$ -integrin. The effect of  $\alpha 3$ -integrin KO was determined on Schaffer-collateral-CA1 synapses. Electrophysiological recordings were performed on  $f(\alpha 3)$ KO [Cre/+;  $f(\alpha 3)/f(\alpha 3)$ ] and control [Cre/+; +/+ and +/+;  $f(\alpha 3)/f(\alpha 3)$ ] animals. (A) Input/output curves revealed a small but significant decrease in basal synaptic transmission between the two sibling controls at higher stimulus intensities ( $F_{(4,30)} = 21$ ,  $P < 0.0001$ ). The basis for this difference is unknown. Most importantly, no significant differences were observed between the Cre/+; +/+ control and the  $f(\alpha 3)$ KO animals. All subsequent experiments were performed using a stimulus intensity that elicited a fEPSP with a slope that was 50% of the maximum fEPSP slope, normalizing for any subtle differences in basal synaptic transmission. (B) No significant differences due to genotype were observed in neurotransmitter release as assessed with paired pulse facilitation ( $F_{(2,85)} = 1.2$ ,  $P > 0.3$ ). (C) No significant differences were observed in the short-term form of plasticity, post-tetanic potentiation ( $F_{(2,21)} = 1.8$ ,  $P > 0.2$ ). (D) Induction of LTP using a modest stimulus paradigm (two 1-sec stimuli at 100 Hz separated by 20 sec) revealed a significant deficit in the  $f(\alpha 3)$ KO mice relative to their Cre/+; +/+ and +/+;  $f(\alpha 3)/f(\alpha 3)$  littermates ( $F_{(2,39)} = 88$ ,  $P < 0.0001$ ). (E) LTP induced by a robust stimulus paradigm (four 1-sec stimuli at 100 Hz separated by 5 min) was impaired in  $f(\alpha 3)$ KO slices ( $F_{(2,6)} = 35$ ,  $P < 0.05$ ). (F) Measurement of the area under the curve for each tetanus in the robust LTP induction paradigm indicated no significant differences, suggesting the synaptic mechanisms involved in induction of LTP are unimpaired in  $f(\alpha 3)$ KO mice ( $F_{(2,7)} = 0.25$ ,  $P > 0.8$ ). (G) Induction of mGluR-LTD in the  $f(\alpha 3)$ KO mice was not significantly different from littermate control genotypes, indicating that loss of  $\alpha 3$  at Schaffer-collateral-CA1 synapses does not inhibit induction and/or expression of synaptic plasticity in general ( $F_{(2,47)} = 42$ ,  $P > 0.05$ ).

## Working memory is impaired in $f(\alpha 3)$ KO mice

We next examined the role of  $\alpha 3$ -integrin in learning and memory by assessing the performance of the  $f(\alpha 3)$ KOs in a battery of behavioral tasks. In the rotarod test, which assesses the animal's sensorimotor coordination and motor skill learning ability, the  $f(\alpha 3)$ KO mice showed no difference from the control animals in both the initial performance and the improvement over trials during the course of the experiment (Fig. 4A).

In the open field test, which is a hippocampus- and basal ganglia-dependent task that measures locomotor and exploratory activity of the animal in a novel environment, the  $f(\alpha 3)$ KO mice performed indistinguishably from the control animals, as indicated by the total distance traveled by the animals in each 5-min bin within each 30-min interval (Fig. 4B). The similar decrease in the activity during each interval indicated that the  $f(\alpha 3)$ KO animals had the same ability to habituate to a novel environment as did the control animals. In both the mutant and the control groups, the reduced level of activity by the end of the first trial was similarly retained after the 30-min intertrial interval (ITI) and at the start of the second trial, indicating no obvious difference in the memory of habituation in the  $f(\alpha 3)$ KO mice. In addition, the ratio of time spent near the edges of the open field arena versus the center was equivalent between the  $f(\alpha 3)$ KO animals and the controls (data not shown), indicating that no difference in anxiety level was detectable by this measure.

We next examined the performance of the knockout mice using the Morris watermaze assay, a hippocampus-dependent task that measures the ability of the animal to acquire spatial reference memory. Both the  $f(\alpha 3)$ KO and the control animals improved their escape latency (Fig. 4D) and path lengths taken (data not shown) at a similar rate over 5 d of training, indicating that the knockout animals were normal in their ability to acquire the spatial task. To test whether the reference memory of the knockout animals was intact, we performed probe trials 24 h (Fig. 4D,E) or 1 wk (data not shown) after the last training trial. The results showed that spatial memory in the  $f(\alpha 3)$ KO animals was indistinguishable from the controls at both time points.

Previously, we have shown that animals with a forebrain-specific knockout of  $\beta 1$ -integrin, the only known  $\beta$ -integrin partner for  $\alpha 3$ -integrin, exhibit impaired working memory in the nonmatch-to-place T-maze assay. We

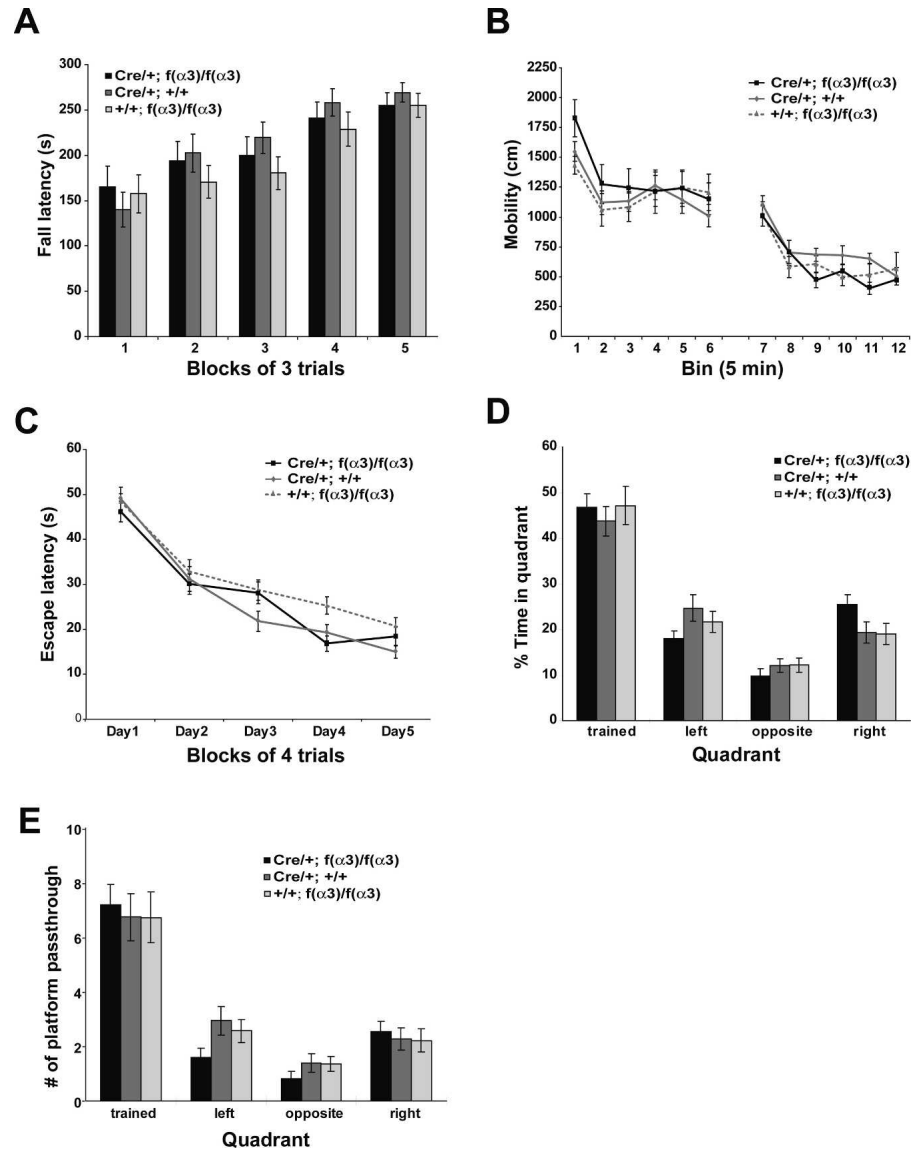


**Figure 4.**  $\alpha 3$ -Integrin knockouts exhibited normal behavioral performance in rotarod, open field, and water maze tasks. (A) Latency to fall as a function of trial block in the rotarod task. All three groups of animals showed significant improvement in their latency to fall in this task over 5 d of training ( $F_{(21,29)} = 233$ ,  $P < 0.0001$ ). No significant difference was detected in the performance between the genotypes on any day ( $P > 0.88$ ). (B) Locomotor activity in the open field. The  $f(\alpha 3)$ KO mice showed no difference in activity from the controls in each 5-min bin ( $F_{(2,41)} = 0.169$ ,  $P = 0.85$ ). Like the controls, the  $f(\alpha 3)$ KO mice showed a significant reduction in activity 5 min after entering the open field in each of the two sessions (bin 1 vs. bin 2,  $P = 0.0003$ ; bin 7 vs. bin 8,  $P = 0.03$ ), indicating that the knockout animals showed normal habituation. In addition, all groups retained a habituated level of activity across the 30-min interval between the two sessions (bin 6 vs. bin 7), suggesting no difference in the memory of habituation between the genotypes. (C) Acquisition of spatial memory plotted as escape latency as a function of training day in the hidden version of the water maze. No significant difference was observed between the  $f(\alpha 3)$ KO ( $Cre/+; f(\alpha 3)/f(\alpha 3)$ ,  $n = 15$ ) and the control groups ( $Cre/+; +/+$ ,  $n = 15$ ;  $+/+; f(\alpha 3)/f(\alpha 3)$ ,  $n = 14$ ;  $F_{(2,41)} = 0.788$ ;  $P = 0.46$ ; ANOVA with repeated measures). (D) Percentage of time spent in each quadrant during a probe trial at 24 h after the last training trial. (E) Number of platform crossings during the probe trial at 24 h after the last training trial. For both D and E, the  $\alpha 3$ -integrin knockout and the control groups spent significantly more time in the trained quadrant than in the other three quadrants ( $P \leq 0.01$  for each genotype; Scheffé's post hoc comparison) and passed through the platform location in the trained quadrant significantly more times than that in the other quadrants ( $\leq 0.01$  for each genotype; Scheffé's post hoc comparison). However, no significant difference was found between the knockout and the control groups by both measurements ( $P \geq 0.80$  for each quadrant).

therefore investigated whether  $\alpha 3$ -integrin is also a critical molecule involved in this working memory task. Our results showed that the  $f(\alpha 3)$ KO animals were able to learn and perform as well

as the controls, reaching the criterion (75% correct choices over 20 trials in the choice run; see Materials and Methods). As shown in Figure 5, the performance of the  $f(\alpha 3)$ KO animals after reaching criterion remained indistinguishable from the controls when tested with no delay between the sample and the choice runs. However, the  $f(\alpha 3)$ KO animals performed significantly poorer than did the control animals when a 20-sec delay was imposed between the two runs. This level of behavioral performance was also significantly lower than their performance with no delay, while in contrast, the control animals showed no such decrease in performance with a 20-sec delay over the no delay groups. When the delay was extended to 1 min, the  $f(\alpha 3)$ KO and the control animals performed significantly poorer than their performance with no delay, but at a level that was indistinguishable from their initial performance at the start of the training, indicating the transient nature of memory in this delay, non-match-to-place task. It is noteworthy that there was no significant difference between the performance of the  $f(\alpha 3)$ KOs with a 20-sec and 1-min delay. These results, which were replicated in a second independent experiment with a different set of animals, together with the similar decrease in the working memory performance from  $\beta 1$ -integrin knockouts (Chan et al. 2006), suggest that the  $\alpha 3\beta 1$ -integrin heterodimer is likely the integrin molecule that functions in maintaining the stability of memory in working memory stores.

## Discussion

The current study was undertaken to extend our understanding on the roles of integrins in synaptic plasticity and memory formation. Previously, we presented data showing that a loss of  $\beta 1$ -integrin in the excitatory neurons of the adult mouse forebrain results in impaired basal synaptic transmission and NMDA receptor-dependent LTP, as well as a selective deficit in working memory. No deficits in spatial learning, fear conditioning, motor

learning, or open field habituation were observed for the  $\beta 1$ -integrin forebrain knockouts. However, since the  $\beta 1$ -integrin is known to be the binding partner for several different  $\alpha$ -integrin subunits, the identity of the  $\alpha$ -integrins that function with  $\beta 1$ -integrin for normal basal synaptic transmission, LTP, and working memory remained a critical unknown. In this study we employed genetic tools to selectively remove  $\alpha 3$ -integrin expression in excitatory neurons of the postnatal forebrain and observed a deficit in LTP and working memory similar to that observed in the  $\beta 1$ -integrin knockouts, suggesting that  $\alpha 3\beta 1$  is the integrin heterodimer that likely accounts for these two phenotypes in the  $\beta 1$ -integrin knockouts. Presumably, other  $\beta 1$ -binding  $\alpha$ -integrins that are expressed in the forebrain (Pinkstaff et al. 1999) are responsible for the deficits in basal synaptic transmission observed in the  $\beta 1$ -integrin knockouts. We note that forebrain-specific knockouts of  $\alpha 8$ -integrin fail to exhibit any behavioral phenotypes, including the aforementioned working memory phenotype (C.-S. Chan and R.L. Davis, unpubl.), indicating that the phenotypes observed do not emerge with the removal of any type of integrin. Rather, the various types of integrins expressed in the brain are likely to have different roles in neuronal physiology and behavior.

## Integrins are required for LTP

By using function blocking  $\alpha 3$  antibodies, Kramár et al. (2002) showed that  $\alpha 3$ -integrins are involved in the consolidation, but not the induction, of LTP induced by theta burst stimulation. In contrast, our results suggest that  $\alpha 3$ -integrins are additionally involved in the induction phase of LTP induced by HFS stimulation. These differences may be due to the distinct induction protocols that were used and/or to the specificity and effectiveness of reducing endogenous  $\alpha 3$ -integrin function with pharmacological versus genetic tools. Irrespective of these differences, our results add to the growing evidence indicating that integrins regulate LTP in the adult hippocampus. Given the number of molecules and complexity of signaling pathways potentially associated with integrins on both sides of the synaptic membrane, it is currently difficult to know how integrins perform this function. However, one plausible mechanism would involve integrin-modulation of ion channel activity. Bernard-Trifilo et al. (2005) have shown that infusions of integrin-activating RGD-peptides into hippocampal slices cause a twofold increase in the amplitude and duration of NMDA receptor-mediated synaptic currents. This increase is blocked by the Src kinase inhibitor PP2 or by function blocking anti- $\beta 1$  integrin antibodies. A corresponding increase in the tyrosine phosphorylation of NMDA receptor subunits NR2A and NR2B is also observed in the treated hippocampal slices. When synaptoneuroosomes isolated from adult rat forebrain are treated with RGD-peptides or fibronectin, a rapid increase in a  $\beta 1$  integrin-dependent protein tyrosine phosphorylation was observed for the integrin-related signaling proteins focal adhesion kinase (FAK), proline-rich tyrosine kinase 2 (PYK2) and Src family kinases (Bernard-Trifilo et al. 2005). Thus, integrin signaling modulates NMDA receptor channel activity via downstream tyrosine phosphorylation events. Moreover, RGD-peptides enhance the slope and amplitude of the excitatory post-synaptic responses by modulating AMPA-type glutamate receptors, and this enhancement is blocked by a mixture of function blocking antibodies against integrin  $\alpha 3$ ,  $\alpha 5$ , and  $\alpha V$  subunits; the NMDA receptor antagonist APV; the CaMKII inhibitor KN-93; or the Src tyrosine kinase inhibitor PP2 (Kramár et al. 2003). It has also recently been demonstrated that forebrain conditional  $\beta 1$ -integrin knockouts have impaired basal excitatory synaptic transmission through AMPA receptors at the same Shaffer collateral pathway (Chan et al. 2006). Taken together, these results suggest that binding of some  $\beta 1$ -integrins can enhance the NMDA- and

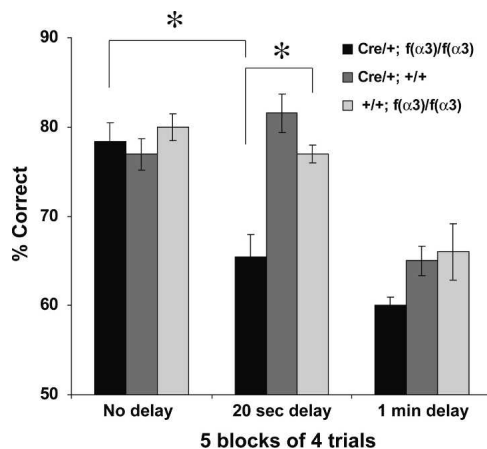


**Figure 5.** The  $\alpha 3$ -integrin knockouts exhibited impaired working memory in a nonmatch-to-place T-maze assay. Working memory was expressed as the percentage of correct choices made during the choice run when performed immediately, 20 sec or 1 min after the sample run. For the statistical analyses, we performed a two-way ANOVA with the main effects of genotype and delay (genotype  $F_{(2,32)} = 3.175$ ,  $P = 0.06$ ; delay  $F_{(2,32)} = 23.68$ ,  $P < 0.0001$ ; interaction  $F_{(4,64)} = 2.87$ ,  $P = 0.03$ ), followed by post-hoc Scheffe's test, which showed a significant effect only between the  $Cre/+$ ;  $f(\alpha 3)/f(\alpha 3)$  vs.  $Cre/+$ ;  $+/+$  ( $P = 0.001$ ) and  $Cre/+$ ;  $f(\alpha 3)/f(\alpha 3)$  vs.  $+/+$ ;  $f(\alpha 3)/f(\alpha 3)$  ( $P = 0.02$ ) at 20-sec delay, and no significant genotype effect at other delays ( $P > 0.48$ ). ( $Cre/+$ ;  $f(\alpha 3)/f(\alpha 3)$ ,  $n = 14$ ;  $Cre/+$ ;  $+/+$ ,  $n = 15$  and  $+/+$ ;  $f(\alpha 3)/f(\alpha 3)$ ,  $n = 13$ ). Similar results were obtained in an independent experiment with a second group of animals (data not shown). Asterisks (\*) represent significant differences. Data represent mean  $\pm$  SEM.

AMPA-receptor function through the activation of the Src/FAK/PYK2/CaMKII kinase signaling cascade.

Alternatively, integrins may modulate LTP through interaction with actin cytoskeleton. In neurons, actin filaments are highly concentrated in dendritic spines, and the reorganization of actin cytoskeleton is known to be involved in regulating the synaptic plasticity. For instance, stimuli that induce LTP spur a rapid and persistent increase in F-actin content within the dendritic spines (Fukazawa et al. 2003; Lin et al. 2005; Kramár et al. 2006), and manipulations that blocked the induction of LTP or reversed LTP within minutes after it was induced disrupted the increase in F-actin content (Lin et al. 2005; Kramár et al. 2006). Furthermore, inhibition of actin filament assembly in the hippocampus by various agents such as latrunculin and cytochalasin impair LTP induced by both HFS and theta burst stimulation, especially during consolidation at the late phase (Kim and Lisman 1999; Krucker et al. 2000; Fukazawa et al. 2003). These effects on LTP produced by blocking actin cytoskeleton assembly are reminiscent of the effects produced by inhibiting integrin function. This provides another plausible mechanism by which integrins modulate LTP, since integrins are known to provide anchor sites for the actin cytoskeleton. Two recent studies support such a hypothesis. Shi and Ethell (2006) have shown that treatment of cultured hippocampal neurons with RGD-peptides induce the elongation of existing dendritic spines and promote the formation of new filopodia. Immunofluorescent labeling of F-actin showed that these effects were accompanied by actin reorganization and synapse remodeling and were mediated by integrins, since they were partially blocked by function-blocking antibodies against  $\beta$ 1- and  $\beta$ 3-integrins. Furthermore, this RGD-induced actin reassembly was suppressed by the NMDA receptor antagonist MK801 and CaMKII inhibitor KN93 as in the integrin-mediated enhancement of AMPA-type currents described above, suggesting that integrins confer structural plasticity of spines through NMDA receptor- and CaMKII-dependent actin reorganization. Kramár et al. (2006) have shown that the actin reassembly caused by LTP-inducing stimulation is blocked by function-blocking antibodies against  $\beta$ 1 integrins when they were applied shortly after the stimulation. Therefore, both the reorganization of the actin cytoskeleton and the expression of LTP require the functions of  $\beta$ 1- (and possibly  $\beta$ 3-) integrins. It is unknown but particularly interesting how actin reassembly is mediated through NMDA receptor/CaMKII signaling, given that integrins are already known to physically link to the actin cytoskeleton through direct and indirect interactions via a large number of bridges.

### Integrins modulate working memory

The results here reinforce our previous finding that integrins are involved in modulating a selective type of memory: hippocampus-dependent working memory. The observed impairment in working memory in the integrin knockouts is not likely due to a motor defect, anxiety, or loss of spatial reference memory, since these animals perform indistinguishably from control animals on tasks that measure these functions. It is noteworthy that although the working memory task employed is hippocampus dependent, our data do not exclude the possibility that integrin function is required in other areas of the forebrain where the Cre recombinase is also expressed (Tsien et al. 1996). Indeed, both  $\beta$ 1- and  $\alpha$ 3-integrin exhibit broad expression in the adult brain (Pinkstaff et al. 1999; Chan et al. 2003). Previous studies with human and non-human primates have indicated that the frontal cortex, parietal cortex, anterior cingulate, and parts of the basal ganglia are crucial for normal working memory (Goldman-Rakic 1995; Smith et al. 1998; Postle and D'Esposito 1999a,b; Skeel et

al. 2001; Lewis et al. 2004; Lenartowicz and McIntosh 2005; Ranganath 2006). Additional experiments are required to further define the precise spatial requirement for integrin function in working memory.

How do integrins modulate working memory? Although it is apparent that the time course for LTP and working memory are distinct, the initial integrin-induced signaling events that lead to the enhanced NMDAR- and AMPAR-mediated synaptic currents during LTP induction as discussed above offers one potential mechanism. Alternatively, although actin-based structural plasticity has been associated with long lasting forms of plasticity and memory (Fukazawa et al. 2003; Lamprecht and LeDoux 2004; Maviel et al. 2004; Lin et al. 2005; Kramár et al. 2006), there is no reason to exclude the possibility that shorter lasting forms of memory may also employ such mechanisms, albeit with changes that may be more modest than those observed during the formation of long-term memory. Indeed, changes in dendritic spine morphology have been observed in electron micrographs as early as 2 min after the induction of LTP (Lamprecht and LeDoux 2004). Recent imaging studies of spine volume after repetitive or LTP-inducing stimulation revealed both rapid (Lang et al. 2004; Matsuzaki et al. 2004) and long-lasting spine enlargement (Matsuzaki et al. 2004), with increases in spine volume being detectable within a minute after stimulation. Increases in spine volume were noticeable in both small and large spines, but persistent long-lasting changes in volume were detectable primarily in spines that were small prior to stimulation.

Working memory, the mechanism that maintains and allows the manipulation of information "on-line" for brief periods of time, is a fundamental cognitive function. Because of this, working memory impairments are frequently observed as an endophenotype in psychiatric and cognitive disorders such as schizophrenia, attention deficit/hyperactivity disorder, and Alzheimer's disease. The discovery of two mouse mutants in integrin genes that exhibit a circumscribed impairment in working memory is most fortunate. There exist dozens of mouse knockouts that impair spatial learning and/or fear conditioning, but there is a dearth of mutants with such circumscribed working memory deficits that provide molecular cues to the biochemical basis for working memory. Two mouse models may be relevant in this respect. Animals that carry a deletion variant in *Disc1*, one of the leading candidate genes for susceptibility to schizophrenia, also exhibit a working memory deficit in a delayed non-match-to-place task (Koike et al. 2006), although electrophysiological studies on these animals have not been reported. *APP<sub>695</sub>SWE* mice, a mouse model for Alzheimer's disease overexpressing a mutated form of amyloid precursor protein, have been shown to exhibit a severe impairment in hippocampal LTP and in working memory as assayed in the delayed non-match-to-place T-maze task when they are old, but not young (Chapman et al. 1999). Interestingly, in contrast to these mice, the behavioral performance of the integrin mutants are observed only when a certain period of delay is imposed, which may suggest that integrins are specifically involved in maintaining the stability, rather than the establishment, of the working memory. Insights on the mechanisms by which integrins are involved in working memory will undoubtedly broaden our understanding of the molecular biology of working memory and perhaps human psychiatric and cognitive disorders.

## Materials and Methods

### Generation of knockout mice

The  $\alpha$ 3-integrin gene was isolated from a BAC library prepared from the 129/SvEv strain. The targeting vector contained 9.4 kb of  $\alpha$ 3-integrin sequence from intron 7 to intron 21 subcloned

into the Bluescript vector (Fig. 1A). The 34-bp loxP sequence was inserted at the BglII site in intron 10, and a 4.9-kb loxP-TK-neo-loxP cassette was inserted at the NheI site in intron 18. The targeting construct DNA was linearized with PvuI and electroporated into 129/SvEv embryonic stem (ES) cells. ES cell clones were selected for neomycin resistance, and homologous recombination was screened by Southern blotting using a 0.8-kb EcoRI fragment 3' of the  $\alpha 3$ -integrin gene. The selected clones were then electroporated with Cre-expressing plasmid, and TK-negative clones were screened by Southern blotting. Two clones were chosen to produce chimeras by microinjection into C57BL/6J blastocysts and implantation into pseudopregnant foster mothers. Chimeric male mice were mated to C57BL/6J females, and offspring that carried the floxed  $\alpha 3$ -integrin [ $f(\alpha 3)$ ] allele were identified by PCR genotyping of tail DNA using the following primer pairs: (1) 5' ATCTGTCTGGTAGCAAAAGGGGTG and 5' TGCTAGCAAAGAAGCTCAGGACTC for the 5' loxP insertion, and (2) 5' CATCTCACCTACACCTTGTGCGGG3' and 5' CACACATCTGTAATCCAAGTGCTC3' for the 3' loxP insertion in the gene. To generate the forebrain-specific  $\alpha 3$ -integrin knockout  $f(\alpha 3)$ KO, the  $f(\alpha 3)$  animals were crossed to T29-1  $\alpha$ -CaMKII-CRE mice. To achieve similar genetic background, both the  $f(\alpha 3)$  and the CRE animals were continuously backcrossed to C57BL/6J mice for over six generations. The  $f(\alpha 3)$ KO animals and the control littermates were obtained by crossing Cre/+;  $f(\alpha 3)$ /+ to +/-;  $f(\alpha 3)$ /+ animals. The presence of the Cre transgene was confirmed by PCR genotyping of tail DNA utilizing the following primers: 5'-GGCGTTTCTGAGCATACTGGAA-3' and 5'-CACCATTGC CCCTGTTCACTATC-3'.

Mice were housed in conventional animal cages and maintained on a 12-h light/dark cycle. All animals were handled and treated during the experiments in ways approved by the Baylor College of Medicine Institutional Animal Care and Use Committee and according to national regulations and policies.

### Electron microscopy of hippocampal area CA1

Twelve- to 16-wk-old animals were anesthetized with isoflurane (50 mg/kg) and perfused transcardially with 0.1 M of phosphate buffer (pH 7.2) followed by a fixative containing 2.5% glutaraldehyde, 2.0% formaldehyde in 0.1 M of cacodylate buffer with 2 mM  $\text{CaCl}_2$ . After post-fixation of the dissected brain overnight at 4°C, the hippocampal CA1 region was dissected and fixed again with 1%  $\text{OsO}_4$  in 0.1 M of cacodylate buffer for 1 h. After washing, the tissue fragments were stained with 1% uranyl acetate for 1 h. The tissue was then dehydrated with an ethanol series and embedded in Glauert Med embedding resin. Ultra-thin sections were cut from the stratum radiatum and visualized with a Hitachi 7500 digital electron microscope. Synapse size was obtained by measuring the length of the post-synaptic density (PSD). Synaptic cleft width was estimated by dividing the area of the cleft juxtaposed to each PSD by the length of that same PSD.

### Hippocampal slice preparation

Twelve to 16-wk-old mice were sacrificed by cervical dislocation and used for all experiments except for the LTD experiments, for which 4- to 5-wk-old animals were used. The brain was immersed in ice-cold cutting saline (CS: 110 mM sucrose, 60 mM NaCl, 3 mM KCl, 1.25 mM  $\text{NaH}_2\text{PO}_4$ , 28 mM  $\text{NaHCO}_3$ , 0.5 mM  $\text{CaCl}_2$ , 7 mM  $\text{MgCl}_2$ , 5 mM glucose, 0.6 mM ascorbate) prior to isolation of the caudal portion containing the hippocampus and entorhinal cortex. Transverse slices (400  $\mu\text{m}$ ) were prepared with a Vibratome (Vibratome). During isolation, slices were stored in ice-cold CS. After isolation, cortical tissue was removed, and hippocampal slices were equilibrated in a mixture of 50% CS and 50% artificial cerebrospinal fluid (ACSF: 125 mM NaCl, 2.5 mM KCl, 1.25 mM  $\text{NaH}_2\text{PO}_4$ , 25 mM  $\text{NaHCO}_3$ , 2 mM  $\text{CaCl}_2$ , 1 mM  $\text{MgCl}_2$ , 25 mM glucose) at room temperature (RT). Slices were further equilibrated in 100% ACSF for 45 min at RT, followed by a final incubation in 100% ACSF for 1 h at 30°C. All solutions were saturated with 95%/5%  $\text{O}_2/\text{CO}_2$ . Slices were treated with the appropriate drugs or vehicle after the last equilibration at 32°C.

### Slice electrophysiology

Electrophysiology was performed in an interface chamber (Fine Science Tools). Oxygenated ACSF (95%/5%  $\text{O}_2/\text{CO}_2$ ) was warmed (30°C, TC-324B temperature controller, Warner Instruments) and perfused into the recording chamber at a rate of 1 mL/min. Electrophysiological traces were amplified (Model 1800 amplifier, A-M Systems), digitized and stored (Digidata models 1200 and 1320A with Clampex software, Molecular Devices). Extracellular stimuli were administered (Model 2200 stimulus isolator, A-M Systems) on the border of Area CA3 and CA1 along the Schaffer-collaterals using enameled, bipolar platinum-tungsten (92%/8%) electrodes. fEPSPs were recorded in stratum radiatum with an ACSF-filled glass recording electrode (1–3 M $\Omega$ ). The relationship between fiber volley and fEPSP slopes over various stimulus intensities (0.5–15 V, 25 nA–1.5 A) was used to assess baseline synaptic transmission. All subsequent experimental stimuli were set to an intensity that evoked a fEPSP that had a slope of 50% of the maximum fEPSP slope. PPF was measured at various interstimulus intervals (20, 50, 100, 200, 300 msec). Long-term potentiation was induced by administering 100 Hz tetani (1-sec duration). A modest LTP induction paradigm consisted of two tetani administered 20 sec apart, while a strong LTP induction paradigm consisted of four tetani administered 5 min apart. LTD was induced by exposing slices to 3,5-(S)-DHPG (50  $\mu\text{M}$ ) for 10 min. Synaptic efficacy was monitored 20 min prior to and 2 h following induction of LTD by recording fEPSPs every 20 sec (traces were averaged for every 2-min interval). The experimenter performing the electrophysiology was blind to genotype or treatment.

### Statistical analysis

I/O relationships were fit with a single exponential equation [ $y = \text{Top} \times (1 - e^{-kx})$ ] and the Top and k parameters were compared for significance using an F test. PPF, PTP, long-term potentiation, tetanus-induced depolarization, and LTD were analyzed using a two-way ANOVA with repeated measures, with post-hoc comparisons performed using the method of Bonferroni. Significance for all tests was set at  $P \leq 0.05$ . Data represent mean  $\pm$  SEM.

### Behavioral assays

All animals were 4–6 mo old when behavioral assays were performed.

#### Rotarod

The rotarod apparatus (type 7650; Ugo Basile) was used to evaluate coordination and motor learning skill of the animals. Groups of five mice were trained on the accelerating rod (3-cm diameter, 30 cm long; 4–40 rpm in 5 min), three trials per day with an ITI of 30 min over a period of 4 d or until they reached plateau performance. Each trial lasted 5 min, and the time the mice spent on the rod without falling was recorded.

#### Open field

Mice were placed in the center of a 60  $\times$  60 cm open arena made of opaque Plexiglass and allowed to move freely under indirect illumination for two 30-min sessions separated by an inter-session of 30 min in the home cage. The surface of the arena was cleaned with 70% ethanol and air-dried between mice. The activity of the animals in the arena was tracked with a ceiling mounted video camera connected to a digital tracking device (VP200, HVS Image). Data were analyzed by the HVS open field software.

#### Water maze

Briefly, mice were handled extensively for 2 wk prior to training in the water maze. The animals were kept in individual cages during training and allowed to acclimatize to the water maze room for 1 h prior to the start of the experiment on each day. Each trial began by placing the mouse into the water facing the wall of the maze, and the animal was allowed to search for the platform until the animal climbed onto the platform or when a



maximum of 60 sec had elapsed. The animal was allowed to remain on the platform for 20 sec before it was returned to its cage. Four trials were performed each day with an ITI of 60 min. Trials were balanced for starting positions and began at either the 12, 3, 6, or 9 o'clock position of the pool. The platform location remained constant for any individual mouse for the duration of the training, but different animals were trained with the platform in different positions to avoid quadrant bias. Animals were trained for 5 d at the same time of each day. Twenty-four hours and/or 1 wk after the last training trial, a probe trial (or transfer test) was administered in which the platform was removed from the pool and animals were placed in a quadrant opposite to the location of the training platform and allowed to swim for 60 sec. The time the mice spent searching for the platform in each quadrant and the number of times the mice crossed the virtual platform location were measured. In all trials, the swimming pattern of the animals was tracked with a ceiling mounted video camera connected to a digital tracking device (VP200, HVS Image), and data were analyzed by the HVS water maze software.

#### T-maze non-match-to-place working memory task

The working memory task was performed as described by Reisel et al. (2002). The T-maze was made of wood and was elevated to a height of 1 m from the floor. It consisted of a start arm (47 × 10 cm) and two identical goal arms (35 × 10 cm), each covered with the bedding used in the animals' home cage environment. Animals were restricted to 1 h of food access per day, which resulted in animals maintaining 85% of their free-feeding weight. The animals were habituated to the maze and to drinking the food reward (50 µL of 50% sweetened, condensed milk) from a small dish (2-cm diameter) for 5 d before testing.

Each test trial consisted of a sample run followed by a choice run. On the sample run, food reward was placed about 3 cm from the end on both goal arms in depression wells, but access to one arm was blocked by a wooden block. A mouse was placed inside an opaque cylindrical tube and transported from the home cage to the end of the start arm, where it was released facing the end wall of the start arm. The animal was allowed to find and drink the food reward in the unblocked goal arm. The animal was then collected into the transfer tube and returned to the end of the start arm, with access into the start arm blocked by a wooden block. The time required for this transfer was less than 5 sec and represented the minimum time lapse between the sample and the choice runs, but was not included in the actual timing of the delay. For the choice run, the wooden block was removed with or without delay and the animal was released to choose either goal arm. The animal was allowed to drink the food reward if it chose the previously unvisited arm. The animal was then returned to the home cage. Four trials with a 20-min ITI were performed on each animal per day for 30 d (only data from the last 15 d were included in Fig. 5). The reward arm for each trial was assigned pseudorandomly, i.e., two times for each goal arm each day but with a different order for each animal. Working memory was expressed as the ratio of correct choices over total choices binned for 20 trials. For the statistical analysis, two-way ANOVA was performed followed by post-hoc Scheffé's test. To confirm the results obtained from the first set of animals, a second, independent cohort was tested which was not trained for any other behavioral task except for the working memory task.

#### Acknowledgments

This work was supported by grants MH60420 (R.L.D.) and MH57014 (J.D.S.) from the National Institutes of Mental Health and the Baylor College of Medicine Mental Retardation Research Center grant HD24064 (R.L.D.). R.L.D. is the recipient of the R. P. Doherty-Welch Chair in Science at the Baylor College of Medicine.

#### References

Bahr, B.A., Staubli, U., Xiao, P., Chun, D., Ji, Z.X., Esteban, E.T., and Lynch, G. 1997. Arg-Gly-Asp-Ser-selective adhesion and the stabilization of long-term potentiation: Pharmacological studies and

- the characterization of a candidate matrix receptor. *J. Neurosci.* **17**: 1320–1329.
- Bernard-Trifilo, J.A., Kramár, E.A., Torp, R., Lin, C.Y., Pineda, E.A., Lynch, G., and Gall, C.M. 2005. Integrin signaling cascades are operational in adult hippocampal synapses and modulate NMDA receptor physiology. *J. Neurochem.* **93**: 834–849.
- Chan, C.-S., Weeber, E.J., Kurup, S., Sweatt, J.D., and Davis, R.L. 2003. Integrin requirement for hippocampal synaptic plasticity and spatial memory. *J. Neurosci.* **23**: 7107–7116.
- Chan, C.-S., Weeber, E.J., Zong, L., Fuchs, E., Sweatt, J.D., and Davis, R.L. 2006.  $\beta$ 1-Integrins are required for hippocampal AMPA receptor-dependent synaptic transmission, synaptic plasticity, and working memory. *J. Neurosci.* **26**: 223–232.
- Chapman, P.F., White, G.L., Jones, M.W., Cooper-Blacketer, D., Marshall, V.J., Irizarry, M., Younkin, L., Good, M.A., Bliss, T.V., Hyman, B.T., et al. 1999. Impaired synaptic plasticity and learning in aged amyloid precursor protein transgenic mice. *Nat. Neurosci.* **2**: 271–276.
- Chun, D., Gall, C.M., Bi, X., and Lynch, G. 2001. Evidence that integrins contribute to multiple stages in the consolidation of long term potentiation in rat hippocampus. *Neuroscience* **105**: 815–829.
- Fukazawa, Y., Saitoh, Y., Ozawa, F., Ohta, Y., Mizuno, K., and Inokuchi, K. 2003. Hippocampal LTP is accompanied by enhanced F-actin content within the dendritic spine that is essential for late LTP maintenance in vivo. *Neuron* **38**: 447–460.
- Goldman-Rakic, P.S. 1995. Cellular basis of working memory. *Neuron* **14**: 477–485.
- Grotewiel, M.S., Beck, C.D., Wu, K.H., Zhu, X.R., and Davis, R.L. 1998. Integrin-mediated short-term memory in *Drosophila*. *Nature* **391**: 455–460.
- Huang, Z., Shimazu, K., Woo, N.H., Zang, K., Muller, U., Lu, B., and Reichardt, L.F. 2006. Distinct roles of the  $\beta$ 1-class integrins at the developing and the mature hippocampal excitatory synapse. *J. Neurosci.* **26**: 11208–11219.
- Hynes, R.O. 2002. Integrins: Bidirectional, allosteric signaling machines. *Cell* **110**: 673–687.
- Kawaguchi, S.Y. and Hirano, T. 2006. Integrin  $\alpha$ 3 $\beta$ 1 suppresses long-term potentiation at inhibitory synapses on the cerebellar Purkinje neuron. *Mol. Cell. Neurosci.* **31**: 416–426.
- Kim, C.H. and Lisman, J.E. 1999. A role of actin filament in synaptic transmission and long-term potentiation. *J. Neurosci.* **19**: 4314–4324.
- Koike, H., Arguello, P.A., Kvajo, M., Karayiorgou, M., and Gogos, J.A. 2006. Disc1 is mutated in the 129S8/SvEv strain and modulates working memory in mice. *Proc. Natl. Acad. Sci.* **103**: 3693–3697.
- Kramár, E.A., Bernard, J.A., Gall, C.M., and Lynch, G. 2002.  $\alpha$ 3 integrin receptors contribute to the consolidation of long-term potentiation. *Neuroscience* **110**: 29–39.
- Kramár, E.A., Bernard, J.A., Gall, C.M., and Lynch, G. 2003. Integrins modulate fast excitatory transmission at hippocampal synapses. *J. Biol. Chem.* **278**: 10722–10730.
- Kramár, E.A., Lin, B., Rex, C.S., Gall, C.M., and Lynch, G. 2006. Integrin-driven actin polymerization consolidates long-term potentiation. *Proc. Natl. Acad. Sci.* **103**: 5579–5584.
- Krucker, T., Siggins, G.R., and Halpain, S. 2000. Dynamic actin filaments are required for stable long-term potentiation (LTP) in area CA1 of the hippocampus. *Proc. Natl. Acad. Sci.* **97**: 6856–6861.
- Lamprecht, R. and LeDoux, J. 2004. Structural plasticity and memory. *Nat. Rev. Neurosci.* **5**: 45–54.
- Lang, C., Barco, A., Zablow, L., Kandel, E.R., Siegelbaum, S.A., and Zakharenko, S.S. 2004. Transient expansion of synaptically connected dendritic spines upon induction of hippocampal long-term potentiation. *Proc. Natl. Acad. Sci.* **101**: 16665–16670.
- Lenartowicz, A. and McIntosh, A. 2005. The role of anterior cingulate cortex in working memory is shaped by functional connectivity. *J. Cogn. Neurosci.* **17**: 1026–1042.
- Lewis, S., Dove, A., Robbins, T., Barker, R., and Owen, A. 2004. Striatal contributions to working memory: A functional magnetic resonance imaging study in humans. *Eur. J. Neurosci.* **19**: 755–760.
- Lin, B., Kramár, E.A., Bi, X., Brucher, F.A., Gall, C.M., and Lynch, G. 2005. Theta stimulation polymerizes actin in dendritic spines of hippocampus. *J. Neurosci.* **25**: 2062–2069.
- Matsuzaki, M., Honkura, N., Ellis-Davies, G.C., and Kasai, H. 2004. Structural basis of long-term potentiation in single dendritic spines. *Nature* **429**: 761–766.
- Maviel, T., Durkin, T.P., Menzaghi, F., and Bontempi, B. 2004. Sites of neocortical reorganization critical for remote spatial memory. *Science* **305**: 96–99.
- Pinkstaff, J.K., Lynch, G., and Gall, C.M. 1998. Localization and seizure-regulation of integrin  $\beta$ 1 mRNA in adult rat brain. *Brain Res. Mol. Brain Res.* **55**: 265–276.
- Pinkstaff, J.K., Detterich, J., Lynch, G., and Gall, C. 1999. Integrin subunit gene expression is regionally differentiated in adult brain. *J.*

- Neurosci.* **19**: 1541–1556.
- Postle, B.R. and D'Esposito, M. 1999a. Dissociation of human caudate nucleus activity in spatial and nonspatial working memory: An event-related fMRI study. *Brain Res. Cogn. Brain Res.* **8**: 107–115.
- Postle, B.R. and D'Esposito, M. 1999b. "What"–Then–Where" in visual working memory: An event-related fMRI study. *J. Cogn. Neurosci.* **11**: 585–597.
- Ranganath, C. 2006. Working memory for visual objects: Complementary roles of inferior temporal, medial temporal, and prefrontal cortex. *Neuroscience* **139**: 277–289.
- Reisel, D., Bannerman, D.M., Schmitt, W.B., Deacon, R.M., Flint, J., Borchardt, T., Seeburg, P.H., and Rawlin, J.N. 2002. Spatial memory dissociations in mice lacking GluR1. *Nat. Neurosci.* **9**: 868–873.
- Rohrbough, J., Grotewiel, M.S., Davis, R.L., and Broadie, K. 2000. Integrin-mediated regulation of synaptic morphology, transmission, and plasticity. *J. Neurosci.* **20**: 6868–6878.
- Shi, Y. and Ethell, I.M. 2006. Integrins control dendritic spine plasticity in hippocampal neurons through NMDA receptor and  $\text{Ca}^{2+}$ /calmodulin-dependent protein kinase II-mediated actin reorganization. *J. Neurosci.* **26**: 1813–1822.
- Skeel, R., Crosson, B., Nadeau, S., Algina, J., Bauer, R., and Fennell, E. 2001. Basal ganglia dysfunction, working memory, and sentence comprehension in patients with Parkinson's disease. *Neuropsychologia* **39**: 962–971.
- Smith, E., Jonides, J., Marshuetz, C., and Koeppel, R. 1998. Components of verbal working memory: Evidence from neuroimaging. *Proc. Natl. Acad. Sci.* **95**: 876–882.
- Stäubli, U., Chun, D., and Lynch, G. 1998. Time-dependent reversal of long-term potentiation by an integrin antagonist. *J. Neurosci.* **18**: 3460–3469.
- Tsien, J.Z., Chen, D.F., Gerber, D., Tom, C., Mercer, E.H., Anderson, D.J., Mayford, M., Kandel, E.R., and Tonegawa, S. 1996. Subregion- and cell type-restricted gene knockout in mouse brain. *Cell* **87**: 1317–1326.
- van der Flier, A. and Sonnenberg, A. 2001. Function and interactions of integrins. *Cell Tissue Res.* **305**: 285–298.
- Wu, L.G. and Saggau, P. 1994. Presynaptic calcium is increased during normal synaptic transmission and paired-pulse facilitation, but not in long-term potentiation in area CA1 of hippocampus. *J. Neurosci.* **14**: 645–654.

Received May 25, 2007; accepted in revised form July 30, 2007.